ARMA 11-417

Visco-plastic properties of shale gas reservoir rocks

Sone, H. and Zoback, M.D.
Stanford University, Stanford, California, USA

This paper was prepared for presentation at the 45th US Rock Mechanics / Geomechanics Symposium held in San Francisco, CA, June 26–29, 2011.

ABSTRACT: We are studying the time-dependent deformational properties of shale gas reservoir rocks through laboratory creep experiments in a triaxial deformation apparatus under room temperature, room humidity conditions. The clay and carbonate content of these shales vary markedly, and the total organic content varies between 1-6%. We find that the constitutive law governing the time-dependent deformation of these rocks is visco-plastic, and the form of the creep constitutive law is described as a power-law function of time. Observations suggest that these rocks are much more susceptible to creep deformation in bedding-perpendicular direction than in bedding-parallel directions. The amount of creep strain increases with sample clay content, regardless of the carbonate content, where a pronounced increase in creep strain occurs at around 35-40% clay content. The amount of creep strain is relatively insensitive to the confining pressure, but increases slightly with differential pressure. Understanding controls on the visco-plastic deformation of these samples is important for designing hydraulic fracturing operations in shale gas reservoirs, since visco-plastic deformation can inhibit brittle deformation during hydraulic fracturing, enhance proppant embedment and permeability reduction after completion, or alter the stress state in the reservoir over geologic time scales.

1. INTRODUCTION

Characterization of the mechanical properties of reservoir rocks often focuses on its elastic properties through sonic log data and laboratory tests on core samples; however, it is also important to understand the time-dependent mechanical properties of these rocks in order to predict the long-term reservoir behavior over production time scales. Many laboratory studies have shown that deformation of unconsolidated reservoir sands and shales occur through elastic-visco-plastic constitutive behavior [1-5], where a significant portion of the deformation takes place by a non-linear response not predicted by linear elasticity. Failing to address the time-dependent response of these reservoir rocks would, for instance, lead to a significant under-estimation of subsidence or permeability reduction of the reservoir.

On the other hand, visco-plastic behavior of more intact reservoir rocks has not received much attention. This is an obvious consequence of the fact that intact rocks exhibit much less time-dependent characteristics compared to unconsolidated rocks, and they appear to behave more or less elastically. Shale gas reservoir rocks are an example of such intact reservoir rocks, amongst others, which we have focused in our study.

We investigate the time-dependent deformational properties of gas shale since they may be related to the in-situ stress heterogeneity observed in gas shale reservoirs. Understanding the stress heterogeneity within shale gas reservoirs is crucial to the development of these reservoirs since stimulation by hydraulic fracturing is essential to produce from these low permeability reservoirs, and outcomes of fracturing procedures are greatly influenced by the in-situ state of stress. A study [6] shows that the occurrence of drilling-induced borehole failure observed through FMI image logs correlate with the fluctuation in the lithology within the reservoir (i.e. fluctuation in clay, carbonate content), which suggests that the stress heterogeneity is controlled by the mechanical heterogeneity within the reservoir. Some studies approach this problem by appealing to the heterogeneity in elastic properties [7], but there is no doubt that the long-term visco-plastic behavior of the reservoir rock plays a significant role in determining the in-situ state of stress (e.g. stress perturbation around ductile salt domes). Our objective is to characterize the visco-plastic behavior of shale gas reservoir rocks through laboratory experiments using shale samples from various shale gas reservoirs.

2. METHODS

2.1. Sample Description

Samples used in the laboratory experiments come from four different gas shale reservoirs: Barnett shale, Haynesville shale, Fort St. John shale, and Eagle Ford

shale. The mineralogy and the total organic content of all samples are characterized by powder XRD analyses and Rock Eval pyrolysis, except for the Eagle Ford shale sample (Table 1). Samples from Barnett shale and Haynesville shale are further divided in to two sub-groups, dark and light, to reflect the differences in clay content between the two sub-groups. Samples were kept under room humidity condition prior to the test and experiments were performed under dry and pore pressure drained condition. Although mechanical behaviors of clay minerals are known to change with water saturation [8], we chose to conduct our experiments under room-dry conditions to eliminate poro-elastic effects that may mask the visco-plastic behavior of the dry framework that we are studying. All samples were shaped to cylindrical plug samples of diameter 25.4 mm (1 inch) and length ranging between 28-54 mm. Axes of the cylindrical plugs were either parallel or perpendicular to the bedding plane, referred to as horizontal and vertical samples, respectively.

Table 1. Sample groups and its compositions in percent. QFP refers to quartz, feldspar, plagioclase, and pyrite component.

Sample group	Clay	Carbonate	QFP	TOC
Barnett-dark	30-45	0-6	48-61	4.0-5.8
Barnett-light	2-7	39-81	16-53	0.4-1.3
Haynesville-dark	34-43	21-29	34-38	2.8-3.2
Haynesville-light	22-24	51-54	23-26	1.7-1.8
Fort St. John	34-42	3-6	54-60	1.6-2.2
Eagle Ford	n/a	n/a	n/a	n/a

2.2. *Experimental Procedures*

Plug samples were tested for its time-dependent deformational properties in a triaxial apparatus (Autolab2000, New England Research Inc.) under hydrostatic and triaxial loading conditions. Axial and radial deformations were measured by two pairs of individual sensors, and the confining pressure and differential load on the sample were monitored by a pressure gauge and an internal load cell, respectively, during the experiments.

A typical experiment is performed in 3 stages, hydrostatic, triaxial and failure & friction, as shown in Figure 1. Samples were subject to several steps of isotropic confining pressures, P_c, in the hydrostatic stage, after which the pressure was held constant for 3-6 hours to observe any possible hydrostatic creep deformation. After each pressure holds, the pressure was decreased and increased over several minutes before proceeding to the next pressure step, in order to measure the elastic modulus. After all of the pressure steps, confining pressure reached between 20-60 MPa. We do not report results from the hydrostatic stage though, since significant amounts of creep strain was not observed during hydrostatic loadings except for in the Haynesville-dark samples.

In the triaxial stage, the differential pressure, $P_{diff}=P_a-P_c$, was increased in two to four steps while holding confining pressure constant at 20-60 MPa. Differential load was held constant after each step change in axial pressure to observe creep deformation, for 3 hours to 2 weeks at the longest, and un-/reloaded to measure the elastic constants. The magnitudes of the differential loads were chosen to reach about 50% of the rock strength after all steps, so as not to observe tertiary creep, or "brittle creep", that ultimately leads to the failure of the rock [9].

Finally in the failure and friction stage, the sample was taken to failure by loading the sample in the axial direction at a constant strain rate of about 10^{-5} s^{-1}. This allowed us to measure the ultimate strength and sliding friction of the rock.

Several stress relaxation tests were also conducted, in which the axial strain was held constant rather than the differential axial pressure during the triaxial stage. Such tests help to characterize the governing constitutive behavior of the visco-plastic deformation.

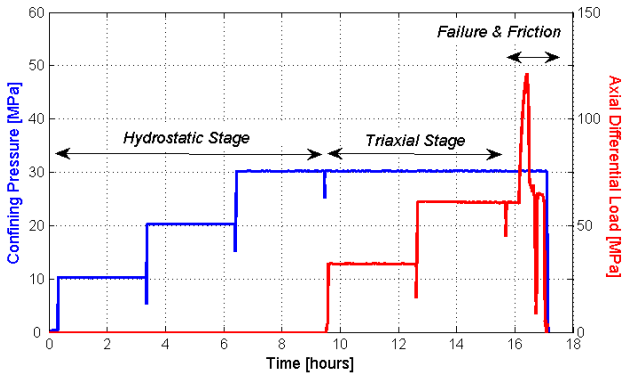

Figure 1. The confining pressure and axial differential load during a typical experiment.

3. RESULTS

3.1. *Time Dependence*

In order to characterize the time-dependent mechanical behavior of the rocks at production time-scales, it is ultimately recommended that observations be made at the same time scale. However this is usually not possible in a laboratory. In our case, 3 hours was the feasible time we could accommodate to routinely observe creep, but we also observed several weeks-long creep to address the issue of extrapolating 3-hour creep data to longer time scales. Figure 2 shows an example of such long-duration creep observed over 2 weeks at 20 MPa confining pressure and 30 MPa differential stress for a Haynesville-light sample.

In figure 2, a logarithm and power-law function is fit to the data before 10^4 seconds, which roughly corresponds to 3 hours. The form of the logarithm and power-law functions are:

$$\varepsilon_{creep} = A\log(t) \quad (1)$$

$$\varepsilon_{creep} = Bt^n \quad (2)$$

where A, B, and n are constants. If we were to only consider the earlier stage of the creep up to 3 hours, we might conclude that a logarithm function better describes the creep behavior from the apparent linear trend between logarithm of time and creep strain [10]. However, it is evident from the later stage creep data that a power-law function captures the long-term behavior better. Therefore, we chose to fit a power-law function to all of our creep data between 10^2-10^4 seconds to analyze and compare data, although the beginning of the creep is not well described by a power-law function.

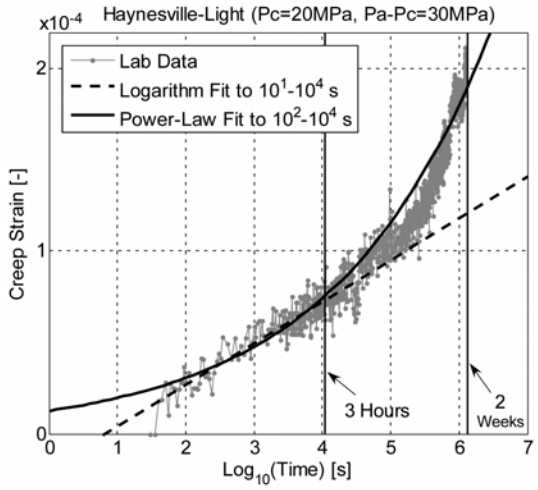

Figure 2. Long-duration creep data compared with a logarithm and power-law function.

3.2. *Creep during Cyclic Loading*

In order to understand whether the observed creep deformation is recoverable or not, thus whether it is elastic or plastic, we also performed an experiment where pressure was held constant for an extended period of time after step pressure unloading as well. Figure 3 shows the creep strain observed for a Haynesville-dark sample at 30 MPa confining pressure under cyclic differential pressure steps between about 0-35 MPa. We see that there may be a slight rebound in creep strain after unloading of differential pressure, but majority of the creep strain seen during the initial loading of the sample is not recovered. Upon reloading of differential pressure to the same level as the previous loading, creep resumes as if it is continuing from where it left off. Therefore, the time-dependent creep behavior we observe in our experiments is best characterized as being visco-plastic, with a slight visco-elastic component.

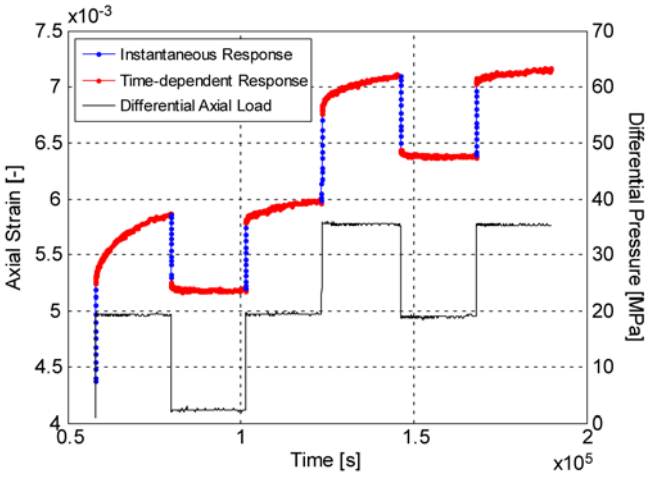

Figure 3. Creep after loading, unloading, and re-loading. Sample is Haynesville-dark at P_c=30 MPa

3.3. *Pressure Dependence*

Figure 4 plots the amount of creep strain observed after 3 hours of constant stress load against the differential pressure applied for all samples tested. Although some samples experienced different pressure loading histories rather than the typical "3-hour hold per step" routine, it is observed consistently that creep strain increases with increasing differential pressure. Note that data from the same sample group was collected under different confining pressure conditions, but significant differences are not observed within a group. Thus, creep strain is dependent on differential stress but not sensitive to the confining pressure. It is also observed that the relation between creep strain and differential stress extends down close to the origin except for the Haynesville-dark samples. This is perhaps consistent with the fact that Haynesville-dark was the only group that exhibit noticeable creep strain during the hydrostatic stage. In fact, hydrostatic (axial) creep in Haynesville-dark samples ranged between 2-4*10^{-4}, which seems to be close to the intercept of the trend between axial creep strain and differential stress with the vertical axis.

We have also compared the power-law exponent, the *n*-values, that were obtained by fitting Eq. (2) to each laboratory data in figure 5. It is difficult to admit any trend in the data, but we recognize that most values fall within the range 0.15-0.25 and values are similar with each other within a sample group, except for Barnett-light and Eagle Ford samples. This apparent scatter in the *n*-values seen in these samples mainly reflects the low signal-to-noise ratio in the data. Barnett-light and Eagle Ford samples exhibit creep strain of less than 10^{-4} after 3 hours which is comparable to the magnitude of the noise. Thus the scatter in the *n*-values is probably

mainly due to error in fitting the power-law function. The fact that *n*-values tend to be more confined at higher differential pressure supports this notion, because the error in regression is expected to be smaller at higher differential pressure where the magnitude of creep is larger and the signal-to-noise ratio improved. Therefore it may be a general conclusion that *n*-values fall in between 0.15-0.25.

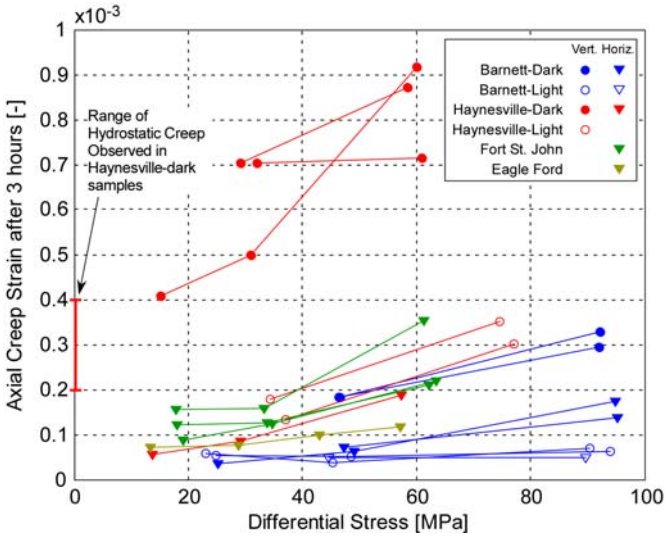

Figure 4. Creep strain versus differential stress.

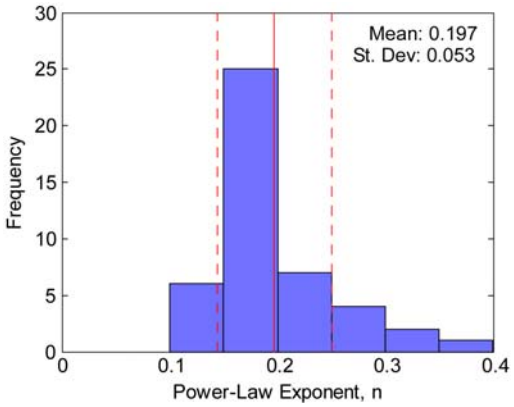

Figure 5. Histogram of the power-law exponent, n, determined from each creep data.

There is a wide variation in the amount of creep observed between samples. From figure 4, we see that the orientation of the stress relative to the bedding plane has a significant influence. Creep strain in the direction perpendicular to the bedding can be several factors larger than in the direction parallel to the bedding.

Comparing the amount of creep against their mineralogy also shows that clay content is the strongest control on the amount of creep amongst other constituents (figure 6). By comparing plots from the vertical samples only, we see that creep strain increases with clay content with a marked increase at about 35-40% clay content. Horizontal samples also follows the same trend, although much subtle, where creep increases with clay. It is noted that comparison against other components such as carbonate or TOC does not produce a monotonic relation as with the clay content.

Comparison of creep strain against other mechanical properties shows that elastic moduli, particularly the Young's modulus, correlate fairly well with the tendency to creep (figure 7). On the other hand, the Poisson's ratio does not correlate with the amount of creep strain.

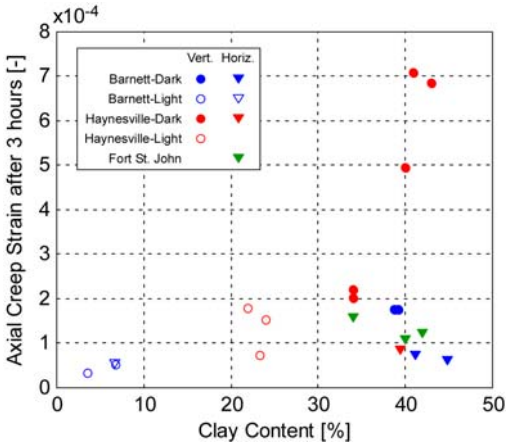

Figure 6. Creep strain versus clay content. The creep data obtained at differential stress closest to 40 MPa is taken to represent a sample.

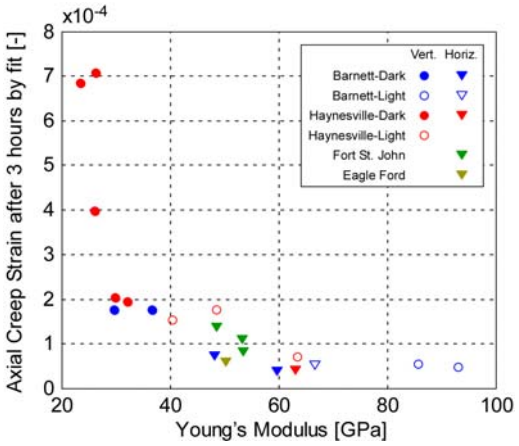

Figure 7. Creep strain versus Young's modulus. The creep data obtained at differential stress closest to 40 MPa is taken to represent a sample.

3.4. Stress Relaxation Tests

Examples of results from the stress relaxation tests are shown in figure 8. Axial stress, P_a, was controlled so as to produce a step change in axial strain and then maintain that axial strain over 3 hours. As a result, the differential stress increases instantaneously and then decays over time as plastic deformation takes place within the sample in a time-dependent fashion. Such stress relaxation response was interpreted in the log-log domain, and we find that the stress relaxation also follows a power-law relationship between time and stress. Stress relaxation tests were performed for all sample groups except the Eagle Ford shale, and we find

that the power-law exponent for the stress relaxation ranges in between -0.01 to -0.05, an order of magnitude smaller than those for creep tests.

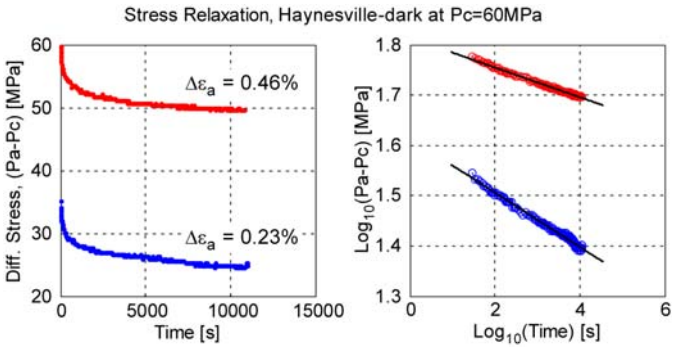

Figure 8. Stress relaxation data from a Haynesville-dark sample tested at 60 MPa confining pressure. The right panel is the same data as the left panel but plotted in log-log space.

3.5. Intact Rock Strength and Sliding Friciton

Rock strength and sliding friction measured from the final stage of the experiments are shown in Figure 9. As seen in the plots, uniaxial compressive strength and sliding frictional coefficient correlates well with clay contents. Rocks with higher clay content are weaker.

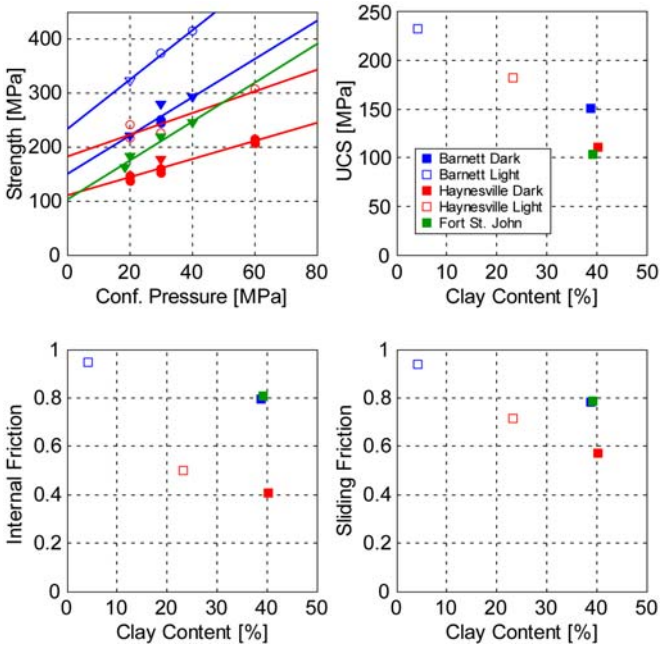

Figure 9. UCS, internal friction, and sliding friction plotted against clay content. The top left panel shows the linear regression against strength data which was used to determine UCS and internal friction.

4. DISCUSSION

4.1. Constitutive Relations

Our experiments show that the creep behavior of the tested shale gas reservoir rocks can be expressed as a power-law function of time as expressed in Eq. (2), at least within the time scales tested. For the purpose of simplifying the argument, we interpret figure 5 to be showing that the power-law exponent, n, is identical for all samples tested, somewhere between 0.15-0.25. In such case, the amount of creep strain after a given time is controlled by the magnitude of constant B in Eq. (2). As seen in figure 4, amount of creep strain depends on the differential pressure exerted to the sample. Amount of creep is also controlled by the sample mineralogical composition, namely its clay content, and the sample orientation, and the combined effect of these two factors seem to be proxied fairly well by the static Young's modulus of the sample (figure 7). Thus, constant B should be a function of differential stress and Young's modulus, resulting in a general expression of creep as:

$$\varepsilon_{creep} = B\left(P_{diff}, E_{static}\right) * t^{n} \qquad (3)$$

While Eq. (3) could be useful to predict creep behavior of shale gas reservoir rocks if the functional form of $B(P_{diff}, E_{static})$ is constrained by fitting lines or curves to the data in figures 4 and 7, it only describes the creep response to a single step load in differential stress. It would be much useful if one can predict the time-dependent strain response of the rock against an arbitrary stress history. Next, we treat the creep behavior in the framework of visco-elasticity to discuss such possibility.

4.2. Comparison with Visco-Elasticity

Visco-elasticity has been applied to geological materials to characterize the time-dependent deformation or dispersion/attenuation behavior of unconsolidated sediments [3,11]. Although these material and the shale gas reservoir rocks we tested actually possess visco-plastic material behavior, visco-elasticity could be a useful framework for analyzing the time-dependent characteristic of these rocks.

A fundamental principle that underlies the theory of visco-elasticity is the Boltzmann superposition principle. If the relaxation modulus, E(t), and the creep compliance, J(t), is the stress and strain response, respectively, against a step input of the other, Boltzmann superposition states that the stress response to an arbitrary input of strain history is equal to the convolution of the relaxation modulus, E(t), against the strain-rate history. The parallel argument also holds, so that the strain response to an arbitrary input of stress history is obtained by convolving the creep compliance, J(t), against the stress-rate history [12]. A useful outcome of these two statements is that one can analytically determine the E(t) by knowing the J(t), or vice versa, by some mathematical treatments utilizing the Laplace and inverse Laplace transformations [11,12].

Following such argument, if a visco-elastic material possesses a power-law creep compliance function of the

form Eq. (2), one can determine the corresponding relaxation modulus to be of the form:

$$\sigma_{relaxation} = Ct^{-n} \quad (4)$$

Where C is a constant and n is the same value as the power-law exponent in the original creep compliance function. Thus, if we can experimentally observe that the power-law exponent of the creep compliance function and the relaxation modulus function is identical in magnitude, we understand that the material follows visco-elastic behavior, in which the stress/strain response to an arbitrary input of strain/stress, can be predicted from the knowledge of only the E(t) or the J(t). However, our experimental data shows that the power-law exponent for the creep compliance generally falls between 0.2±0.05, whereas the power-law exponent for the stress relaxation range between -0.01 to -0.05. Therefore our 3 hour stress relaxation data does not suggest viscoelastic behavior of the samples at this point.

However, further careful treatment of the laboratory data is needed to reach a reliable conclusion on this matter. We understand that our stress relaxation tests may not have strictly held the strain of the sample constant during the experiments. Our apparatus was capable of maintaining the axial distance constant between fixed points on the end-caps, which host the sample assembly, rather than the strain directly measured on the sample. Thus as stress relaxed, the end-caps expanded elastically, and, in return, the sample must have undergone some axial shortening which may have inhibited the relaxation of stress to a certain degree. If such scenario is true, the magnitude of the power-law exponent in the stress relaxation response may actually be larger than what we observed.

Also we may need to include the instantaneous elastic response of the rock in the creep compliance function, in which case analytical derivation of the corresponding relaxation modulus function is not trivial if not impossible. There is also a slight inaccuracy in the treatment of the data due to the finite time it takes to produce a load step at the beginning of the creep. These issues will require numerical determination of the creep compliance and relaxation modulus functions from the laboratory data. Further experiments/ analyses are needed in order to address whether simplification of the viscoplastic behavior by viscoelastic theory is valid or not.

4.3. Implications for In-situ State of Stress

While the exact constitutive formulation is yet unknown for the time-dependent mechanical response of the tested shale rocks, it is evident that these shale rocks exhibit varying degrees of viscous responses as seen in the creep behavior. Although the variation in stress relaxation responses is still being investigated, we could expect that stress relaxation response could be quite variable as well amongst the shale samples. If this is true, we could expect that significant stress heterogeneity could be produced via the heterogeneity in lithology within a shale gas reservoir. That is, if a shale gas reservoir with some internal lithological heterogeneity is loaded in the horizontal direction tectonically, layers with different mineral composition would relax the horizontal stress anisotropy by varying degree and/or over varying time scale. Future experiments will further focus on characterizing the relaxation modulus of shale gas reservoir rocks in order to address its effect on in-situ state of stress in these reservoirs.

5. SUMMARY

- Creep deformation of the shale gas reservoir rocks tested follow a power-law function of time
- Majority of the creep deformation observed is plastic.
- The magnitude of creep strain observed under constant differential stress for shale gas reservoir rocks depend on the magnitude of the differential stress applied, the clay content, and the relative orientation of the sample to the stress.
- The static Young's modulus is a good proxy for predicting the magnitude of creep deformation.
- Difference in the visco-plastic behavior of shale gas reservoir rocks within a reservoir is expected to cause in-situ stress heterogeneity.

REFERENCES

1. de Waal, J.A. and Smits, R.M.M. 1985. Prediction of reservoir compaction and surface Subsidence: Field application of a new model. SPE14214
2. Dudley, J.W., M.T. Myers, R.D. Shew, and M.M. Arasteh 1994. Measuring compaction and compressibilities in unconsolidated reservoir materials via time-scaling creep. SPE28026.
3. Chang, C., D. Moos, and M.D. Zoback. 1997. Anelasticity and dispersion in dry unconsolidated sands. *Int. J. Rock Mech. & Min. Sci.* 34(3-4): No.048.
4. Hagin, P.N. and M.D. Zoback. 2007. Predicting and monitoring long-term compaction in unconsolidated reservoir sands using a dual power law model. *Geophysics*, 72(5): E165-E173.
5. Chang, C. and M.D. Zoback. 2009. Viscous creep in room-dried unconsolidated Gulf of Mexico shale (I): Experimental results. *Journal of Petroleum Science and Engineering*, 69, 239-246.
6. Sone, H. and M.D. Zoback. 2010. Stress heterogeneity observed in Barnett Shale, TX, and its relation to the distribution of clay-rich ductile formations. Abstract T21B-2164 presented at 2010 AGU Fall Meeting, AGU, San Francisco, Calif., 13-17 Dec.
7. Suarez-Rivera, R., S.J., Green, J., McLennan, M., Bai. 2006. Effect of layered heterogeneity on fracture

initiation in tight gas shales. SPE103327.
8. Moore, D.E. and D.A. Lockner. 2007. Friction of smectite clay montmorillonite: A review and interpretation of data. In *The Seismogenic Zone of Subduction Thrust Faults.* eds. Dixon, T. H. and J. C. Moore, 317-345.
9. Lockner, D.A. 1993. Room temperature creep in saturated granite. *J. Geophys. Res.*, 98(B1), 475-487.
10. Sone, H. and M.D. Zoback. 2010. Strength, creep and frictional properties of gas shale reservoir rocks. *44th US Rock Mechanics Symposium, Salt Lake City, 27-30 June 2010*, 10-463.
11. Hagin, P.N. and M.D. Zoback. 2007. Viscous deformation of unconsolidated reservoir sands—Part 2: Linear viscoelastic models. *Geophysics*, 69(3), 742-751.
12. Lakes, R.S. 1999. *Viscoelastic solids*: CRC Press.